A study of metabolic compartmentation in the rat heart and cardiac mitochondria using high-resolution magic angle spinning ^{1}H NMR spectroscopy

M.E. Bollard[a], A.J. Murray[b], K. Clarke[b], J.K. Nicholson[a], J.L. Griffin[c,*]

[a] *Biological Chemistry, Biomedical Sciences Division, Imperial College, Sir Alexander Fleming Building, South Kensington, London SW7 2AY, UK*
[b] *University Laboratory of Physiology, University of Oxford, Parks Road, Oxford OX1 3PT, UK*
[c] *Department of Biochemistry, University of Cambridge, Tennis Court Road, Cambridge CB2 1QW, UK*

Received 30 May 2003; revised 20 August 2003; accepted 26 August 2003

First published online 5 September 2003

Edited by Vladimir Skulachev

Abstract High-resolution magic angle spinning (MAS) ^{1}H nuclear magnetic resonance (NMR) spectroscopy is increasingly being used to monitor metabolic abnormalities within cells and intact tissues. Many toxicological insults and metabolic diseases affect subcellular organelles, particularly mitochondria. In this study high-resolution ^{1}H NMR spectroscopy was used to examine metabolic compartmentation between the cytosol and mitochondria in the rat heart to investigate whether biomarkers of mitochondrial dysfunction could be identified and further define the mitochondrial environment. High-resolution MAS spectra of mitochondria revealed NMR signals from lactate, alanine, taurine, choline, phosphocholine, creatine, glycine and lipids. However, spectra from mitochondrial extracts contained additional well-resolved resonances from valine, methionine, glutamine, acetoacetate, succinate, and aspartate, suggesting that a number of metabolites bound within the mitochondrial membranes occur in 'NMR invisible' environments. This effect was further investigated using diffusion-weighted measurements of water and NMR spectroscopy during state 2 and state 3 respiration. State 3 respiration caused a decrease in the resonance intensity of endogenous succinate compared with state 2 respiration, suggesting that coupled respiration may also modulate the NMR detection of metabolites within mitochondria.

Key words: Magic angle spinning; Mitochondrial respiration; Tricarboxylic acid cycle

1. Introduction

High-resolution ^{1}H nuclear magnetic resonance (NMR) spectroscopy of tissue extracts is increasingly being used as a means to profile the metabolic events associated with disease, drug toxicity and genetic manipulation. However, metabolites are partitioned between compartments both on a cellular and subcellular level, and the role of an individual metabolite is often determined by the environment/compartment [1,2]. NMR spectroscopy, both in vivo and in situ, has proven successful at examining metabolic compartmentation and inferring the properties of the compartmental environments. Diffusion-weighted magnetic resonance imaging is routinely used for monitoring cerebral disorders such as ischemia and multiple sclerosis via the changes associated with the diffusion of water, monitoring a combination of change in compartmentation and a change in compartmental environments during these disorders [3–6]. Also, both diffusion- and relaxation-weighted NMR spectroscopies of red blood cells have been successfully used to examine compartmentation of water and metabolites in red blood cells [7,8], with Garcia-Perez and colleagues even detecting the effect of subcellular compartmentation of water between the nuclei and cytosol of chicken erythrocytes [9].

However, the subcellular environment of metabolites may also complicate in vivo and in situ NMR spectroscopy. Examining superfused brain slices, Kauppinen and co-workers [10,11] found that a sub-compartment of cerebral glutamate was not NMR visible, suggesting that either synaptic or mitochondrial glutamate may occur in a restricted environment, possessing a very short spin–spin/transverse relaxation time (T_2), and hence being poorly visible in NMR spectra. Similar observations have been made concerning lactate and taurine in muscle and cardiac tissue [12,13].

One problem associated with in vivo and in situ NMR studies of tissues is that resonances are broadened by dipolar couplings, magnetic inhomogeneity and bulk susceptibility differences. Magic angle spinning (MAS) ^{1}H NMR circumvents these problems by averaging these effects to zero when a sample is spun at an angle of 54.7° [14]. Furthermore, the cytoplasm in tissues provides an ideal environment for the application of MAS ^{1}H NMR spectroscopy at modest spin speeds (3–7 kHz), as the environment is more closely liquid than solid phase, allowing molecules to 'tumble', hence reducing intermolecular dipolar coupling [15–17]. For samples which are heterogeneous in terms of magnetic susceptibility, static magnetic field inhomogeneity across the samples at the macroscopic and microscopic level is also improved, again sharpening NMR resonances.

Previously, high-resolution MAS ^{1}H NMR has been utilized in assigning the constituents of the liver, kidney, heart and testes [16–19]. In this study we have used high-resolution MAS ^{1}H NMR spectroscopy to investigate subcellular compartmentation in cardiac tissue. Specifically we have examined

*Corresponding author. Fax: (44)-1223-766002.
E-mail address: jlg40@mole.bio.cam.ac.uk (J.L. Griffin).

Abbreviations: ADC, apparent diffusion coefficient; CPMG, Carr–Purcell–Meiboom–Gill; MAS, magic angle spinning; NOESY, nuclear Overhauser effect spectroscopy; T_2, spin–spin/transverse relaxation time; TSP, 3-trimethylsilyl-1-[2,2,3,3,-$^2H_4$] propionate

0014-5793/03/$22.00 © 2003 Published by Elsevier B.V. on behalf of the Federation of European Biochemical Societies.
doi:10.1016/S0014-5793(03)00969-4

the metabolic components of intact cardiac tissue, intact mitochondria, tissue extracts and mitochondrial extracts. To further characterize mitochondria we have also investigated mitochondrial function in situ using high-resolution MAS ^{1}H NMR spectroscopy.

2. Materials and methods

2.1. Necropsy procedure

All animal procedures conformed to Home Office (UK) Guidelines. Hearts were removed from healthy male Sprague–Dawley rats immediately after killing. Tissue was either snap-frozen using liquid nitrogen and stored at −80°C prior to NMR analysis of intact tissue or extracts, or used immediately to prepare mitochondria.

2.2. Mitochondrial preparation

Hearts were perfused with ice-cold 70 mM sucrose buffer at pH 7.0 containing 220 mM mannitol, 5 mM MOPS and 2 mM ethyleneglycol-bis-(β-aminoethylether)-*N*,*N*,*N*′,*N*′-tetraacetic acid (EGTA) to remove the blood. A second perfusion was carried out with a 10 mg/ml nagarse solution in sucrose buffer after which the ventricular tissue was weighed and minced in 10 ml of nagarse solution. Fresh nagarse solution was added and the tissue homogenized with an equal volume of protease inhibitor solution (1 protease inhibitor cocktail tablet/25 ml sucrose buffer). The remaining homogenate was centrifuged at $900\times g$ for 3 min at a temperature of 4°C prior to decanting of the supernatant and centrifuging at 10,000g for 10 min at 4°C. The pellet was resuspended in 1 ml of sucrose buffer then centrifuged at $15\,000\times g$ for 5 min and a temperature of 4°C. The pellet was washed in 1 ml of 10 mM potassium phosphate buffer, pH 7.4, containing 140 mM of potassium chloride, for 5 min at 4°C, the supernatant discarded and the pellet stored at −80°C.

2.3. Conventional ^{1}H NMR spectroscopy of heart tissue and mitochondrial extracts

Heart tissue samples ($n=5$, ~100 mg) were extracted in acetonitrile and H_2O (50:50; 1 ml to 100 mg of tissue; pH 7) using a sonicating micro-probe (five times 10 s). Samples were centrifuged at $5000\times g$ for 5 min and the solvent removed by freeze drying. For extraction of mitochondrial metabolites, the mitochondrial pellets ($n=5$) were added to phosphate buffer (10 mM NaH_2PO_4/Na_2HPO_4 buffer in 50% D_2O; ~100-fold dilution, pH 7.4). Samples were sonicated for three times 5 s using a micro-probe, prior to centrifugation at 45 000 rpm ($100\,000\times g$) for 90 min. The resulting supernatant was then freeze dried. Extracts were reconstituted in 800 μl of D_2O with 4 mM 3-trimethylsilyl-1-[2,2,3,3,-$^2H_4$] propionate (TSP) and NMR data were acquired on a Bruker DRX600 spectrometer operating at 600.13 MHz ^{1}H observation frequency (Bruker Biospin, Rheinstetten, Germany) using the BEST™ (Bruker efficient sample transfer) flow injection probe for sample delivery and analysis. ^{1}H NMR spectra were acquired with a sweep width of 12 019 Hz for 128 scans using the nuclear Overhauser effect spectroscopy (NOESY) PR1D pulse sequence for water suppression with an acquisition time of 2.73 s and 'mixing time' of 150 ms. This pulse sequence is based on the start of the two-dimensional (2D) NOESY sequence and suppresses B_0 and B_1 effects as well as the water resonance (spectra represent typical results over five replicates unless stated otherwise).

2.4. High-resolution MAS ^{1}H NMR spectroscopy of intact heart tissue and mitochondria

Samples of heart tissue ($n=5$, ~10 mg) were placed in zirconium oxide 4 mm diameter rotors together with 10 μl of D_2O with 4 mM TSP to act as a field frequency lock and chemical shift reference, and analyzed by high-resolution MAS ^{1}H NMR spectroscopy at 600.13 MHz, a temperature of 300 K and a spin rate of 4500 Hz. Spectra were acquired with the NOESY PR1D sequence described above. To reduce the contribution of broad lipid resonances in these spectra, Carr–Purcell–Meiboom–Gill (CPMG) spectra, consisting of a train of 180° spin echoes used to attenuate resonances according to T_2 [20] were also acquired with 256 scans and continuous wave irradiation for solvent suppression. The total spin–spin relaxation delay ($2n\pi$) was varied between 50 and 500 ms to provide spectra with different T_2 weightings as described in Section 3. For assignment purposes, 2D gradient correlation spectroscopy (COSY) spectra were measured on selected samples using 16 transients per increment for 256 increments into 2K data points. A spectral width of 7184 Hz was used with a gradient duration of 1 ms.

For high-resolution MAS ^{1}H NMR spectroscopy of intact mitochondria the above procedure was repeated with 10 μl of ~10 mg of fresh mitochondria in D_2O (previously stored on ice after preparation). Spectra were acquired at either 600.13 (descriptive studies of mitochondria, $n=3$) or 400.13 MHz (for respiration state studies, $n=3$ preparations) using a high-resolution MAS rotor and identical pulse sequences as those described above. Mitochondria were considered viable if the respiratory control ratio was greater than 6 as measured using oxygen consumption rates in conjunction with a Clark electrode, for state 2 respiratory rate (substrate but no adenosine diphosphate (ADP) present) = ~10 nmol O_2 uptake/min/mg protein; state 3 respiratory rate (oxidation of glutamate/malate coupled with adenosine triphosphate (ATP) production) = 70–80 nmol O_2 uptake/min/mg protein). To examine mitochondria in different respiration states, mitochondria were also studied in the presence of 10 μl of D_2O containing 0.25 mM sucrose, 4 mM glutamate, 2 mM malate, 3 mM Mg-acetate, 3 mM potassium phosphate, 0.4 mM EGTA, and 20 mM HEPES, with and without 350 μM ADP for state 3 and 2 respiration, respectively.

2.5. Diffusion-ordered spectroscopy (DOSY) of intact mitochondria

For diffusion spectroscopy a stimulated echo pulse sequence incorporating bipolar gradients as described by Wu and colleagues [21] was used with 32 increments of a 53.1 Gauss/cm field gradient placed along the magic angle axis. Sine-shaped gradients of duration 2 ms ($\delta/2$ for a bipolar sequence) were used with 50, 100, 200 or 300 ms inter-gradient delays. Thirty-two transients were acquired for each increment using a 16 k time domain over a spectral width of 8.4 kHz. The apparent diffusion coefficient (ADC) of water was computed by fitting the NMR signal as a function of gradient strength squared into a single or double exponential within XWINNMR (version 3.1, Bruker GmBH, Germany).

3. Results and discussion

The spectra of conventional cardiac tissue extracts contained sharp resonances from many low molecular weight metabolites including lactate, alanine, acetate, glutamate, glutamine, succinate (not visible at current magnification), creatine, taurine, choline and adenosine (not shown), as well as resonances due to short chain lipids soluble in the acetonitrile/water extraction medium (Fig. 1). By comparison, high-resolution MAS ^{1}H NMR spectra of cardiac tissue were dominated by resonances associated with lipids, especially saturated groups such as $H_2CH_2CH_2$ and H_2CH_3 at 1.29 and 0.89 parts per million (ppm) (bold type signifying which resonances are observed; Fig. 1). However, using 2D NMR spectroscopy (Fig. 2), resonances were assigned for all the low molecular weight metabolites found in the 1D spectra of tissue extracts as well as threonine and lysine, indicating that most of the metabolites extracted from cardiac tissues using an aqueous extract procedure are NMR visible using high-resolution MAS ^{1}H NMR spectroscopy.

Table 1
ADC of water in a sample of suspended mitochondria measured with four different inter-gradient delays (Δ)

Diffusion delay/ms	Exponential fit/$\times 10^{-10}$ m^2 s^{-1}	Average translational path/μm
50	12.2 ± 3.1	11
100	9.4 ± 0.3	14
200	7.5 ± 0.2	17
300	5.4 ± 0.2	18

$n=3$. The average translational path (σ) of water was calculated by $\sigma\sim\sqrt{}(2*\Delta*\mathrm{ADC})$ for $\Delta\gg\delta$ where δ is the time the gradient is applied for [9].

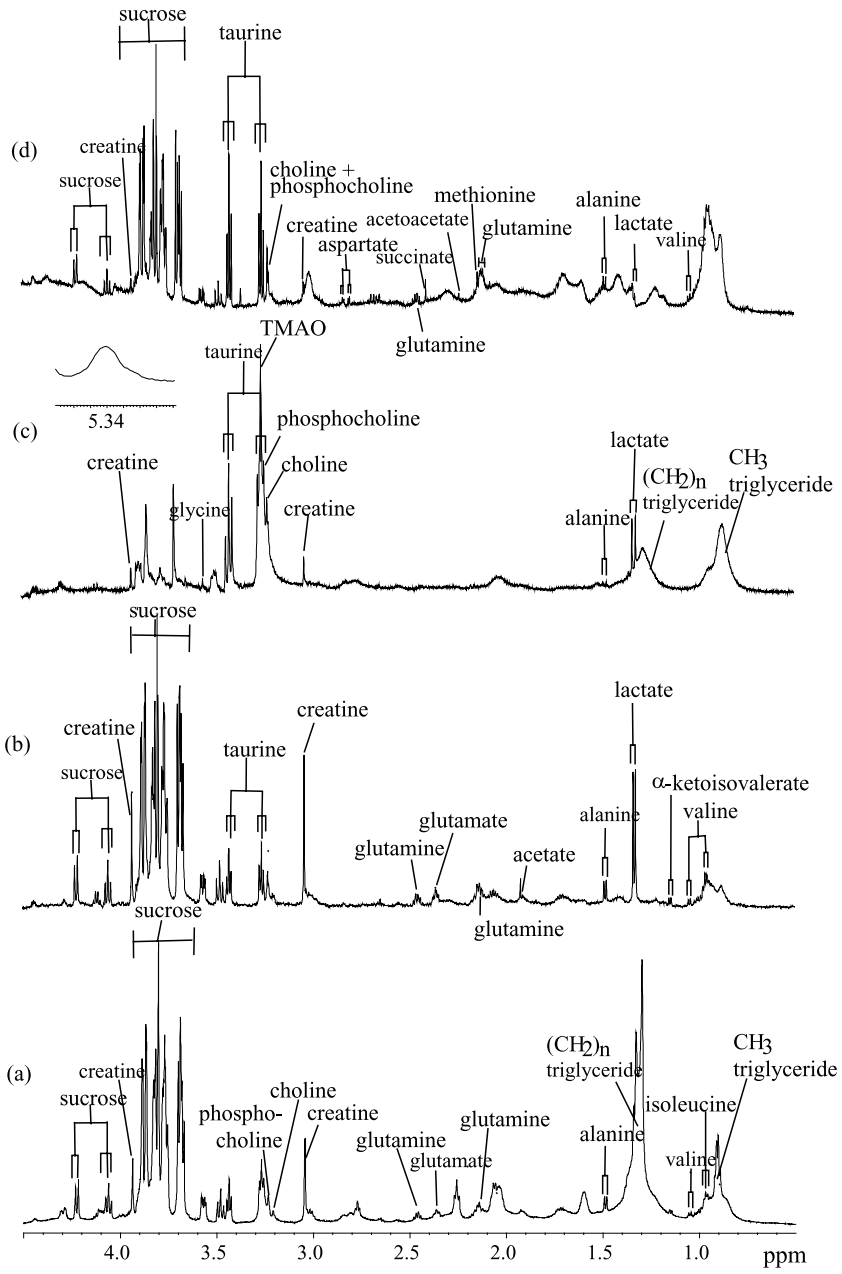

Fig. 1. 600.13 MHz ^{1}H NMR solvent suppressed spectra. a: High-resolution MAS ^{1}H NMR spectrum of intact rat cardiac tissue. b: NMR spectrum of an extract of rat cardiac tissue. c: High-resolution MAS ^{1}H NMR spectrum of rat heart mitochondria. d: NMR spectrum of an extract of rat heart mitochondria. Insert shows CH=CH resonance detected in c.

Spectra of mitochondrial extracts (Fig. 1) contained many sharp resonances from low molecular weight metabolites including valine, methionine, glutamine, acetoacetate, succinate, aspartate, creatine, and choline. Observing the metabolites contained within mitochondria directly, high-resolution MAS ^{1}H NMR spectra of rat heart mitochondria largely reflected lipid resonances including the resonances at 2.71 and 5.35 ppm from $CH=CHCH_2CH=CH$ and CH=CH moieties in polyunsaturated fats (PUFAs) (Fig. 1). While the spectra contained sharp resonances from taurine, choline, phosphocholine, glycine and creatine these resonances made only a small contribution to the spectra compared with the lipid resonances (Fig. 1), suggesting that many of the metabolites detected in extracts of mitochondria are in a highly restricted environment within intact mitochondria.

Using a stimulated gradient echo to attenuate the water resonance according to the diffusion properties of water, attenuation curves were found to fit to a monoexponential function for the four diffusion times used with $R^2 > 0.95$. The calculated ADC for water was less than that for free water and decreased with increasing diffusion time (Δ), consistent with the water being in a restricted environment (Table 1). However, calculating the average translational path of water for each diffusion time, indicated a mean free path, an order of magnitude larger than mammalian mitochondria which are $\sim$1 μm in length. This suggests the water attenuation detected was the result of water both extra- and intra-mitochondrial, producing a single component as a result of rapid averaging of these environments, so that the ADC of water represented an average of the two extremes. The dynamics

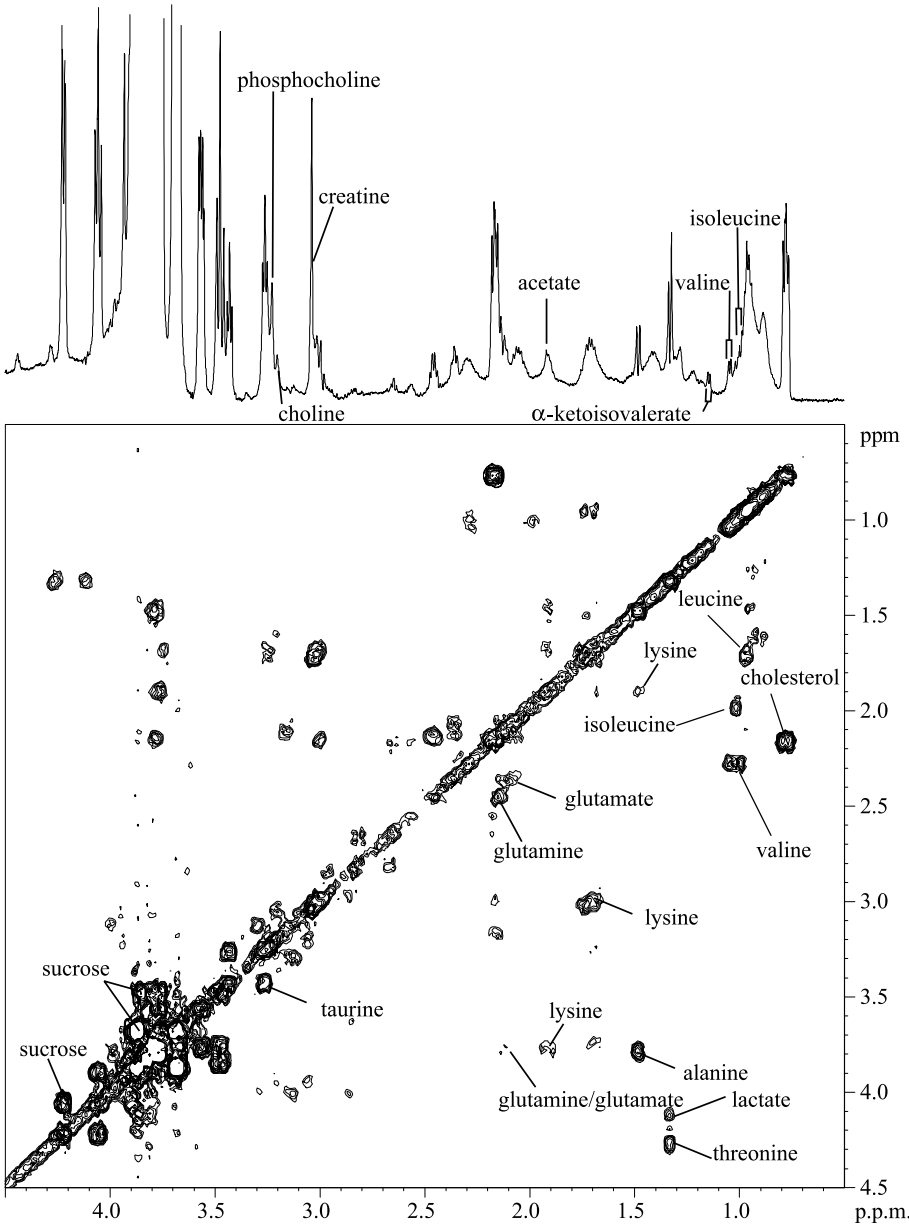

Fig. 2. 600.13 MHz gradient. ^{1}H-^{1}H COSY high-resolution MAS NMR spectrum of rat heart tissue.

and environment of water in suspensions of isolated rat liver mitochondria have been previously investigated by ^{1}H NMR using T_1 and T_2 relaxation as a probe. Results showed mono-exponential relaxation in resuspension medium and in mitochondrial suspensions, suggesting a fast water exchange across the inner mitochondrial membrane [22]. To investigate the mitochondrial environment further, fresh mitochondria were incubated in HEPES buffer containing glutamate and malate with or without ADP ($n = 3$). As previously observed, conventional spectra of the mitochondria had a relatively large contribution from lipid resonances. Using a CPMG pulse sequence with a spin echo delay of 200 or 500 ms to partially and completely attenuate all the lipid and HEPES, respectively, the singlets from succinate and acetate at 2.4 and 1.9 ppm were detectable. The increase in spin echo times produced a narrower resonance for succinate, with a linewidth of 10 Hz using a 200 ms total spin echo and 4 Hz using a 500 ms total spin echo. Standardizing spectra to the acetate resonance, the succinate singlet at 2.4 ppm was reduced in intensity for mitochondria resuspended in the presence of ADP compared to those without, with state 3 respiration producing $11 \pm 4\%$ and $25 \pm 8\%$ decrease in the resonance integral using a 200 or 500 ms spin echo ($n = 3$) (Fig. 3).

High-resolution MAS ^{1}H NMR spectroscopy of intact tissue maintains tissue structure and allows the observation of spectra comparable in resolution to those obtained in solution state [14–16], facilitating investigations into metabolic compartmentation in situ. However, there have been numerous reports of NMR invisible metabolite pools, including compartments of ADP, lactate, creatine, glutamate and taurine existing in highly restricted environments [10–13]. In the present study, the detection of a number of organic acids and amino acids, including acetoacetate and glutamine, in the mitochondrial extracts, but not in intact mitochondria,

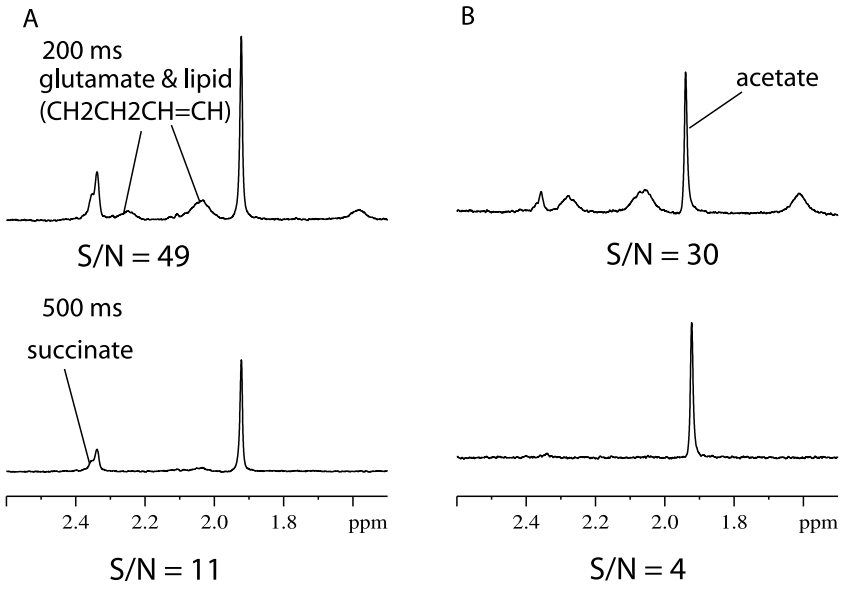

Fig. 3. 400.13 MHz CPMG high-resolution MAS ^{1}H NMR spectra of mitochondria using a total spin echo delay of 200 ms (top spectra) or 500 ms (bottom spectra). Spectra are scaled according to the intensity of the acetate peak at 1.9 ppm. Key: A: Mitochondria incubated with malate and glutamate only. B: Mitochondria incubated with malate, glutamate and ADP. S/N signifies the signal to noise ratio for the succinate peak in each spectrum.

suggests that a number of metabolites within mitochondria occur in 'NMR invisible' environments, and even low molecular weight metabolites that are detected by high-resolution MAS spectroscopy may have resonances that are underrepresented in terms of their total mitochondrial concentration.

The internal environment of the mitochondrion is highly viscous, and molecules will have low mobility and hence short T_2. In addition, the mitochondrion contains numerous paramagnetic moieties, particularly the complexes of the respiratory chain, which will lead to line broadening of NMR resonances. Haggie and Brindle [23], investigating the visibility of ^{19}F labelled proteins within mitochondria, found that while free citrate synthase labelled using ^{19}F fluorine tagged tryptophan was readily observable in vitro, in yeast mitochondria none of the ^{19}F resonances normally detectable could be observed. Line broadening as a result of the high viscous nature of mitochondria and sequestration of enzymes into multienzyme complexes was thought to be responsible for this. In a similar manner metabolites may be complexed with enzymes within the mitochondrial matrix. Analogously, the free concentration of ADP in the cytosol, as detected by NMR spectroscopy, is significantly smaller than that measured using extraction procedures as a result of ADP complexation with proteins within the cytosol [24,25].

Unfortunately, it was not possible to deduce anything directly about the mitochondrial environment of water, with the rapid transport of water most likely confounding our measurements so that only one diffusion component was detected at each diffusion delay. However, Cerdan and colleagues [9] investigating the diffusion properties of water in liver mitochondria have measured an ADC for mitochondrial water of $5.8 \pm 1.9 \times 10^{-10}$ m^2 s^{-1} using a biexponential fit, demonstrating a relatively restricted environment and comparable to the value measured in this study using a diffusion delay of 300 ms. However, they used shorter diffusion times than those that were applied in this study and exchange of water across the mitochondrial membrane may have had a smaller contribution to their attenuation profiles.

To further investigate the effects of NMR visibility on metabolites within mitochondria, state 2 and 3 respirations were investigated using ^{1}H NMR spectroscopy. High-resolution MAS ^{1}H NMR spectroscopy of the pellet of mitochondria failed to detect the resonances from malate, despite the use of a CPMG filter to attenuate the resonances of HEPES, suggesting the substrate was transported within the mitochondria. A broad resonance at 2.1 ppm may have contained a contribution from glutamate, but again line broadening processes, presumably due to the restricted environment within the mitochondria, made this difficult to assess. However, singlets at 8.35 and 8.26 ppm were detectable in these spectra indicating that ADP and/or ATP were observable. The decrease in the resonance intensity of endogenous succinate during state 3 as compared with state 2 respiration suggests that coupling of oxidative phosphorylation to the redox transport chain causes a repartition of succinate between an NMR observable and an NMR invisible pool. Intriguingly this was also accompanied by an increase in the resonance intensity of the broad resonances at 2.1 ppm suggesting that glutamate may have become more visible. Robinson and colleagues [26], investigating the competition for oxaloacetate, produced by malate dehydrogenase (MDH), between aspartate amino transferase (AspAT) and either cytosolic or mitochondrial citrate synthase (CS) in vitro, discovered that mitochondrial CS outcompeted AspAT while the reverse was true for AspAT and cytosolic CS. They suggested a multienzyme complex was formed between mitochondrial CS and MDH, with the oxaloacetate channelled between the two enzymes. In this study, the decrease in succinate could result from its conversion to malate via fumarate which in turn is complexed with a mitochondrial multienzyme metabolic arrangement. Alternatively, succinate may become sequestered at the inner mitochondrial membrane with complex II during state 3 respiration, reduc-

ing the rotational freedom of the metabolite as well as placing it in a highly inhomogeneous magnetic environment.

The creatine detected by high-resolution MAS ^{1}H NMR spectra is presumably localized within mitochondrial creatine kinase, found on the outer surface of the inner mitochondrial membrane, possibly coupled to the adenine nucleotide translocase. Thus, the creatine detected is most likely in the intermembrane space, along with other substrates such as lactate which are not transported across the inner mitochondrial membrane.

The lipids detected within mitochondria contained more unsaturated moieties both in terms of mono- and polyunsaturated fats than cardiac tissue as a whole. These same CH=CH and CH=CH–CH_2–CH=CH moieties have been observed to increase in intensity during programmed cell death in glioma [27,28]. Given that apoptosis is triggered by large releases of cytochrome *c* from the mitochondrial membrane, the polyunsaturates detected in mitochondrial membranes may also be responsible for the ^{1}H NMR spectroscopy changes detected during programmed cell death, as mitochondrial lipids become repartitioned into the cytosol.

References

[1] Patel, A.J. and Balazs, R. (1969) Biochem. J. 111, 17P–18P.
[2] Lue, P.F. and Kaplan, J.G. (1970) Biochim. Biophys. Acta 220, 365–372.
[3] Merboldt, K.D., Bruhn, H., Frahm, J., Gyngell, M.L., Hanicke, W. and Deimling, M. (1989) Magn. Reson. Med. 9, 423–429.
[4] Sevick, R.J., Kucharczyk, J., Mintorovitch, J., Moseley, M.E., Derugin, N. and Norman, D. (1990) Acta Neurochir. Suppl. (Wien) 51, 210–212.
[5] Pfeuffer, J., Provencher, S.W. and Gruetter, R. (1999) MAGMA 8, 98–108.
[6] Dreher, W., Busch, E. and Leibfritz, D. (2001) Magn. Reson. Med. 45, 383–389.
[7] Rabenstein, D.L., Millis, K.K. and Straus, E.J. (1988) Anal. Chem. 60, 1380A–1391A.
[8] Torres, A.M., Michniewicz, R.J., Chapman, B.E., Young, G.A.R. and Kuchel, P.W. (1998) Magn. Res. Imag. 16, 423–434.
[9] Garcia-Perez, A.I., Lopez-Beltran, E.A., Kluner, P., Luque, J., Ballesteros, P. and Cerdan, S. (1999) Arch. Biochem. Biophys. 362, 329–338.
[10] Kauppinen, R.A. and Williams, S.R. (1991) J. Neurochem. 57, 1136–1144.
[11] Kauppinen, R.A., Pirttila, T.R., Auriola, S.O. and Williams, S.R. (1994) Biochem. J. 298, 121–127.
[12] Schneider, J., Fekete, E., Weisser, A., Neubauer, S. and von Kienlin, M. (2000) Magn. Reson. Med. 43, 497–502.
[13] Griffin, J.L., Williams, H.J., Sang, E. and Nicholson, J.K. (2001) Magn. Reson. Med. 46, 249–255.
[14] Andrew, E.R., Bradbury, A. and Eades, R.G. (1959) Nature 183, 1802.
[15] Garrod, S., Humpfer, E., Connor, S.C., Polley, S., Lindon, J.C., Spraul, M., Connelly, J., Reid, D., Nicholson, J.K. and Holmes, E. (1999) Magn. Reson. Med. 4, 1108–1118.
[16] Millis, K., Maas, E., Cory, D.G. and Singer, S. (1997) Magn. Reson. Med. 38, 399–403.
[17] Tomlins, A., Foxall, P.J.D., Lindon, J.C., Lynch, M.J., Spraul, M., Everett, J. and Nicholson, J.K. (1998) Anal. Comm. 35, 113–115.
[18] Bollard, M.E., Garrod, S., Holmes, E., Lindon, J.C., Humpfer, E., Spraul, M. and Nicholson, J.K. (2000) Magn. Reson. Med. 44, 201–207.
[19] Griffin, J.L., Troke, J., Walker, L.A., Shore, R.F., Lindon, J.C. and Nicholson, J.K. (2000) FEBS Lett. 486, 225–229.
[20] Meiboom, S. and Gill, D. (1958) Rev. Sci. Instrum. 29, 688.
[21] Wu, D., Chen, A. and Johnson, C.S. (1995) J. Magn. Reson. (Ser. A) 115, 260–264.
[22] Lopez-Beltran, E.A., Mate, M.J. and Cerdan, S. (1996) J. Biol. Chem. 271, 10648–10653.
[23] Haggie, P.M. and Brindle, K.M. (1999) J. Biol. Chem. 274, 3941–3945.
[24] Williams, J.P. and Headrick, J.P. (1996) Biochim. Biophys. Acta 1276, 71–79.
[25] Joubert, F., Hoerter, J.A. and Mazet, J.L. (2002) Mol. Biol. Rep. 29, 177–182.
[26] Robinson Jr., J.B., Inman, L., Sumegi, B. and Srere, P.A. (1987) J. Biol. Chem. 262, 1786–1790.
[27] Hakumaki, J.M., Poptani, H., Puumalainen, A.M., Loimas, S., Paljarvi, L., Yla-Herttuala, S. and Kauppinen, R.A. (1998) Cancer Res. 58, 3791–3799.
[28] Hakumaki, J.M., Poptani, H., Sandmair, A.M., Yla-Herttuala, S. and Kauppinen, R.A. (1999) Nat. Med. 5, 1323–1327.